

## Bragg reflection of low-energy positrons from the surface of graphite

E. M. Gullikson\* and A. P. Mills, Jr.

*AT&T Bell Laboratories, Murray Hill, New Jersey 07974*

(Received 29 June 1987)

We observe Bragg peaks in the elastic backscattering probability of monoenergetic positrons from the [0001] surface of highly oriented pyrolytic graphite. The position of most of the peaks can be explained by a plane spacing  $d$ , slightly contracted from the bulk value and a  $+1.4 \pm 0.5$ -eV positron work function for this surface. An unexpected peak at  $kd/\pi=3.5$ , where  $\hbar k$  is the positron momentum, could be due to multiple-scattering effects.

### I. INTRODUCTION

Low-energy positron diffraction (LEPD), first demonstrated by Rosenberg, Weiss, and Canter,<sup>1</sup> has been compared with low-energy electron diffraction (LEED) in trial studies of Cu surfaces.<sup>2,3</sup> It is believed that LEPD should be easier to interpret<sup>1-6</sup> than LEED because (1) the positrons tend to avoid the ion cores and should have a weaker elastic scattering cross section than electrons; (2) the positron inelastic mean free path is shorter than that of electrons; (3) spin-orbit terms are less important for positrons at low energies in low- $Z$  materials; and (4) there is no exchange force for positrons in ordinary matter. The consequence should be that multiple scattering and spin effects are less important for positrons, thus leading to simpler computations.

Detailed computations are required to understand fully the electron or positron diffraction amplitudes and to deduce the structure of the surfaces of metals. Insulators appear to be easier to interpret: The diffraction amplitudes for some alkali halide<sup>7-10</sup> and rare-gas solid<sup>11</sup> surfaces exhibit a series of peaks that can be attributed to Bragg reflection from various crystal planes of spacing  $d$ . The Bragg condition  $kd/\pi=n$ , where  $\hbar k$  is the momentum of the electron or positron, can be satisfied if the particle feels a potential  $V_0$  while it is inside the crystal. This inner potential is on the order of a few eV. The lowest-order Bragg peaks are easily seen by very low-energy positrons, allowing us to deduce with some confidence the value of  $V_0$ , and hence to obtain an estimate for the positron work function  $\phi_+ \approx -V_0$ .

In the present study, we examine positron diffraction from graphite. Although graphite is not an insulator, we observe a series of Bragg peaks that invite simple interpretation. We find that the inner potential is negative, and hence the positron work function is positive. It appears that the outer layers of graphite are slightly contracted compared to the bulk. We are also able to calculate a lower limit on the positron mean free path at one energy from the width of the peak. A large half-order peak suggests that multiple scattering<sup>12</sup> must be taken into account and that a detailed calculation would be useful.

### II. EXPERIMENT

Our experiments were performed using a magnetically guided slow positron beam and ultrahigh-vacuum target chamber. The relevant beam elements are shown schematically in Fig. 1. The positron source was an uncoated 8-mCi deposit of <sup>22</sup>Na in a 5-mm diameter by 10-mm deep cylindrical hole in a 20-mm diameter Cu cylinder. A flux of  $8 \times 10^5$  slow positrons per second was obtained by condensing an approximately 50  $\mu\text{m}$  thick layer of Ne onto the source at about 6 K.<sup>13</sup> The energy resolution of the beam was improved by accelerating the positrons to 5 keV and remoderating<sup>14</sup> them using an ion-bombarded and annealed Ni(100) crystal, cooled to 77 K.<sup>15</sup> A retarding field scan of the resulting slow positron beam is shown in Fig. 2. The beam resolution is  $\Delta E = 27$  meV, the intensity is  $1 \times 10^5 e^+ \text{sec}^{-1}$ , and the beam diameter is 5 mm.

The high-purity, highly oriented pyrolytic graphite

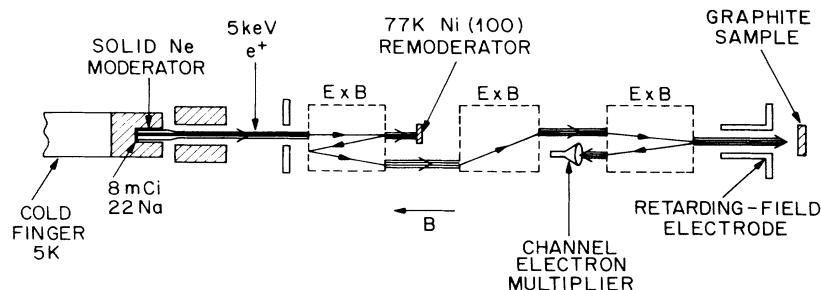


FIG. 1. Neon moderator-Ni(100) remoderator slow positron source and back-reflection LEPD apparatus (not to scale).  $E \times B$  deflectors guide the remoderated narrow energy slow positrons from the Ni crystal to the graphite sample.

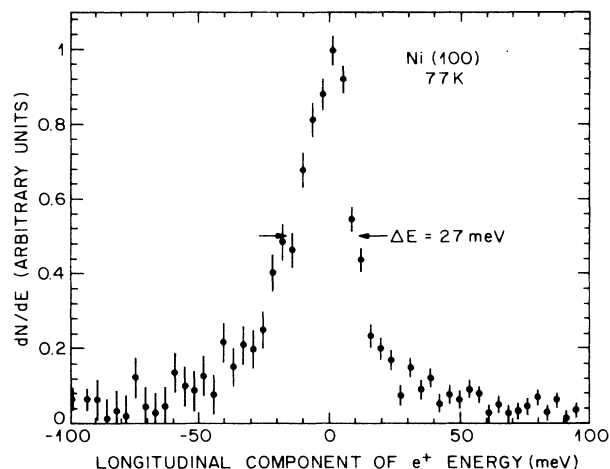


FIG. 2. Distribution of positron kinetic energies parallel to the magnetic induction of Fig. 1. The Ni(100) remoderator was at a temperature of 77 K.

sample was cleaned by heating to  $\approx 900^\circ\text{C}$  *in situ*, and was cooled to  $\approx 50$  K for the LEPD measurements. The incident positron energy was varied by changing the bias on the sample. A retarding-field electrode in front of the sample was biased 0.5 V below the incident positron energy to prevent any positrons from leaving the vicinity of the sample unless they were elastically back-scattered. The back-scattered positrons were detected with a channel electron multiplier, and the counts were recorded in a 1024 channel multiscaler as the sample voltage was swept from  $-10$  to  $+260$  V. The data obtained in a 1 h sweep are shown in Fig. 3. The zero of the energy scale has been shifted to coincide with the point at which positrons are 100% backscattered.

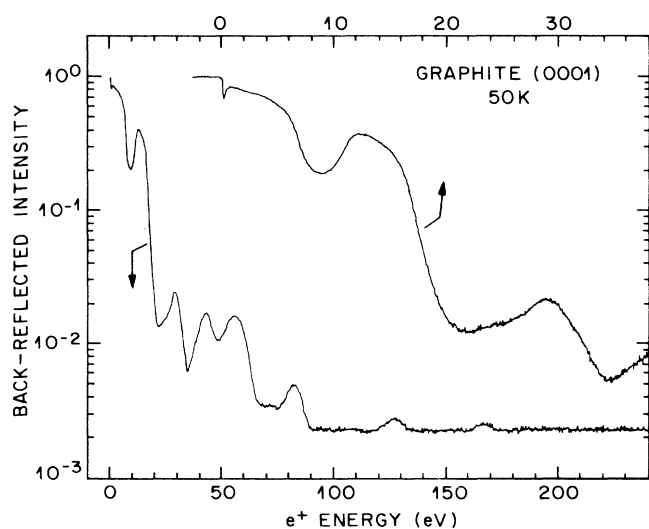


FIG. 3. Positron elastic backscattered intensity vs incident positron kinetic energy for a graphite [0001] surface at 50 K. The upper curve shows the low-energy portion of the plot on a five-times-expanded energy scale.

TABLE I. Peak positions and order number of Bragg reflection.

Peak position (V)	Index ( $n$ )	Fit
13.0	2	12.5
29.0	3	29.9
34.6	(dip)	
42.9	...	
55.8	4	54.2
82.1	5	85.5
127.0	6	123.7
167.8	7	168.9

### III. DISCUSSION

The data of Fig. 3 show a number of peaks that we interpret in terms of Bragg reflection from the crystal planes of graphite. Table I contains a list of the peak locations and the order number of the Bragg reflection that we assign to them. The peak positions are plotted in Fig. 4 versus  $n^2$  and are fitted by the expression

$$E_B = \left[ \frac{12.26}{2d} \right]^2 n^2 + V_0, \quad (1)$$

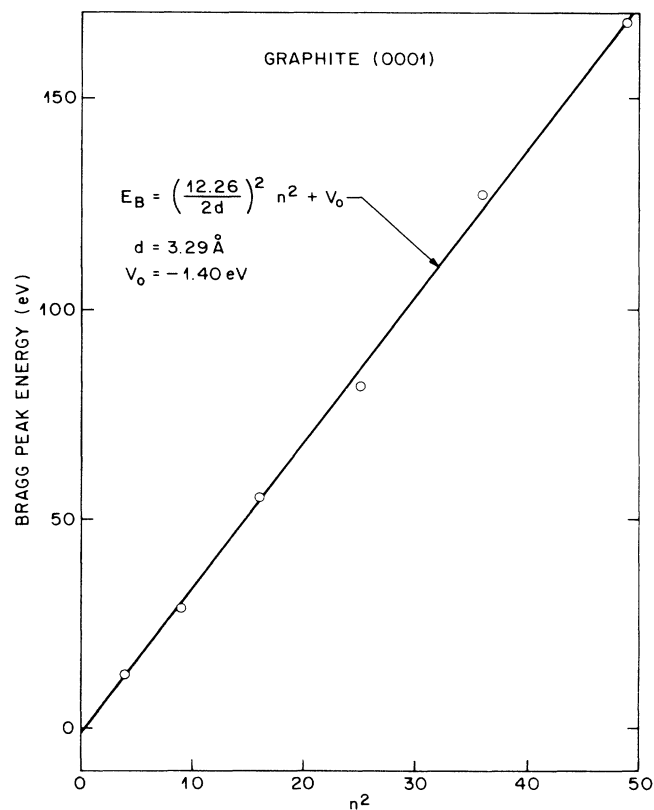


FIG. 4. Positron Bragg peak energies plotted vs the square of the index number  $n$ . The straight line is least-squares fitted to the six data points to obtain an estimate for the inner potential,  $V_0$ , and the lattice constant,  $d$ .

where  $E_B$  is the Bragg energy,  $d$  is the plane spacing, and  $V_0$  is the positron inner potential in eV. The best fit is obtained with  $d = (3.29 \pm 0.02) \text{ \AA}$  and  $V_0 = 1.4 \text{ eV}$ . The lattice parameter of graphite at 50 K,  $c = 6.674 \text{ \AA}$ , would imply  $d = 3.337 \text{ \AA}$ . The dispersion in the residuals (2.6 eV rms) is larger than the precision with which the peak positions are determined.

The Bragg peak structure of the positron elastic back-scattering probability is exhibited in Fig. 5 by plotting the probability as a function of  $kd/\pi$ , where  $k = [2m(E + V_0)/\hbar^2]^{1/2}$  is the positron wave vector in the crystal, and where  $d$  and  $V_0$  were obtained from the fit in Fig. 4. As noted above, the Bragg peaks appear to be shifted slightly from their ideal positions. Furthermore, there is a large unexpected peak corresponding to  $kd/\pi = 3.5$ . These features await explanation by a calculation that includes a realistic positron-carbon atom interaction, multiple-scattering effects, and relaxation of the outer planes of the crystal.

The average value of the crystal potential  $V$  tells us where to locate the bottom of the free-particle energy versus  $\mathbf{k}$  surface in the crystal. The first-order perturbation due to the periodic part of  $V$  introduces energy gaps

$$E^{\text{gap}} = 2V_{\mathbf{G}}, \quad (2)$$

at the zone boundaries,  $\mathbf{k} = \frac{1}{2}\mathbf{G}$ , that we observe as Bragg peaks. Here the  $\mathbf{G}$  are reciprocal lattice vectors, and  $V_{\mathbf{G}}$  are the Fourier expansion coefficients of  $V$ . The second-order perturbation lowers the bottom of the energy surface and the centers of the gaps below the free-particle values by amounts of order  $V_{\mathbf{G}}^2/E_B \approx 1 \text{ eV}$ . Variation of the second-order shifts will thus lead to no more than a fraction of an eV error in our estimate of the bottom of

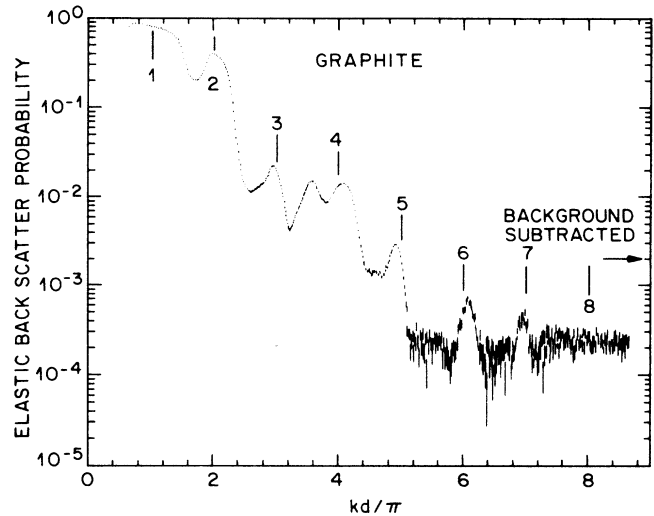


FIG. 5. Data of Fig. 3 plotted vs positron momentum in the crystal.

the energy surface as obtained in Fig. 4. Consequently, our value for the inner potential of graphite is probably equal to the positron affinity within about  $\pm 0.5 \text{ eV}$ . The positron work function is therefore  $\phi_+ = (+1.4 \pm 0.5) \text{ eV}$ .

The width of the Bragg peaks is partly due to the positron band gaps and partly due to attenuation of the positrons. A lower limit on the positron mean free path  $\lambda$  may thus be obtained from the relation  $\lambda = \Delta k^{-1}$ . The fifth Bragg peak is quite narrow, and shows that  $\lambda > 7.8 \text{ \AA}$  for 85 eV positrons, slightly longer than typically observed for electrons at the same energy.<sup>16</sup>

\*Present address: Lawrence Berkeley Laboratories, Berkeley, CA 94720.

<sup>1</sup>I. J. Rosenberg, A. H. Weiss, and K. F. Canter, Phys. Rev. Lett. **44**, 1139 (1980).

<sup>2</sup>A. H. Weiss, I. J. Rosenberg, K. F. Canter, C. B. Duke, and A. Paton, Phys. Rev. B **27**, 867 (1983).

<sup>3</sup>R. Mayer, Chun-Si Zhang, K. G. Lynn, W. E. Frieze, F. Jona, and P. M. Marcus, Phys. Rev. B **35**, 3102 (1987).

<sup>4</sup>R. Feder, Solid State Commun. **34**, 541 (1980).

<sup>5</sup>A. P. Mills, Jr. and P. M. Platzman, Solid State Commun. **35**, 321 (1980).

<sup>6</sup>M. N. Read and D. N. Lowy, Surf. Sci. **107**, L313 (1981).

<sup>7</sup>E. G. McRae and C. W. Caldwell, Surf. Sci. **2**, 509 (1964).

<sup>8</sup>E. G. McRae and C. W. Caldwell, Surf. Sci. **7**, 41 (1967).

<sup>9</sup>A. P. Mills, Jr. and W. S. Crane, Phys. Rev. B **31**, 3988 (1985).

<sup>10</sup>E. G. McRae and R. A. Malic, Surf. Sci. **177**, 74 (1986).

<sup>11</sup>A. Ignatjews, J. B. Pendry, and T. N. Rhodin, Phys. Rev. Lett. **26**, 189 (1971).

<sup>12</sup>E. G. McRae, J. Chem. Phys. **45**, 3258 (1966).

<sup>13</sup>A. P. Mills, Jr. and E. M. Gullikson, Appl. Phys. Lett. **49**, 1121 (1986).

<sup>14</sup>A. P. Mills, Jr., Appl. Phys. **23**, 189 (1980).

<sup>15</sup>B. L. Brown, W. S. Crane, and A. P. Mills, Jr., Appl. Phys. Lett. **48**, 739 (1986).

<sup>16</sup>C. J. Powell, Surf. Sci. **44**, 29 (1974).